Experiments with a Fault Tolerant Adaptive Controller on a Solar Power Plant.
Sixth Portuguese Conference on Automatic Control, June 7-9, Faro, Portugal, 2004.

EXPERIMENTS WITH A FAULT TOLERANT ADAPTIVE CONTROLLER ON A SOLAR POWER PLANT

A. Cardoso[1], P. Gil[1,2], J. Henriques[1], P. Carvalho[1], H. Duarte-Ramos[2], A. Dourado[1]
[1] *CISUC-Informatics Engineering Dep., University of Coimbra,*
Pólo II, 3030-290 Coimbra
[2] *Electrical Engineering Department, UNL, 2829-516 Caparica*
Portugal

Abstract: A fault-tolerant model-based predictive control framework is designed and applied to a Distributed Solar Collector field. The methodology is based on a nonlinear control scheme with a fault diagnosis module. The control system is designed on the basis of a non-linear adaptive constrained model-based predictive control scheme with steady-state offset compensation. The fault detection filter is aimed at providing residual signals, which are subsequently used to identify faults. The controller's robustness and fault tolerance assessment is carried out by injecting faults on the actuator and sensors as well as on the system's parameters.

Keywords: Adaptive control, nonlinear control, model-based control, neural-network models, fault diagnosis, fault tolerance, robustness.

1. INTRODUCTION

In the last few decades model-based predictive control (MPC) methodologies have increasingly received the control community interest and recognition as a valuable approach for solving real control problems. The MPC history can be traced back to the late 1970's with the Model Algorithm Control and the Dynamic Matrix Control techniques (Garcia, *et al.*, 1989). More recently, pushed by the non-linear nature of most industrial processes, some research efforts have been placed in the development of reliable nonlinear model predictive control schemes (NMPC). A well known drawback of "true" NMPC approaches is related to the online solution of a non-convex optimisation problem, as the convergence to a feasible/optimal solution and control system's stability cannot be guaranteed in advanced.

Another issue concerning NMPC is that for many systems it might be difficult or rather expensive to come up with a viable accurate physical model, which is required by all MPC techniques. As an alternative to first principles modelling system's identification can be considered.

Neural networks (NN) have proved to perform quite well in the identification of non-linear systems based on input-output data (see *e.g.* Rivals and Personnaz (1996) and Yamada and Yabuta (1993)). It is well known that neural networks are universal approximators (Hornik, *et al.*, 1989). However, the accuracy of the neural predictor is quite dependent on the quality of the training data set. Furthermore, in the case of offline NN training, a bounded number of iterations and the implementation of regularization techniques may lead to a model/plant mismatch.

As a result, the closed loop system's response will exhibit a steady state offset error. Even in the case of neural network online training this situation might happen due to an adequate adaptation gain. To get around from this effect on the control performance Draeger, *et al.* (1995) suggest adding up to the system's step response an estimate of modelling errors. Another option might be the incorporation in the control loop of a nonlinear offset compensator operating in a narrow range, as proposed in Gil, *et al.* (2000) and Gil, *et al.* (2002).

Regarding the control system's robustness, the incorporation of a fault diagnosis module will contribute to the enforcement of the overall control system fault-tolerance. The fault diagnosis system usually includes the detection, isolation and identification tasks, followed by the fault's accommodation. This module comprises a model-based fault detection filter to generating residual signals in order to detect and isolate eventual faults. The early detection of faults (system malfunctions) combined with a fault-tolerant control strategy can help avoiding the performance degradation of control systems, breakdown and even catastrophes involving human fatalities and material damage (Ichtev, *et al.*, 2002).

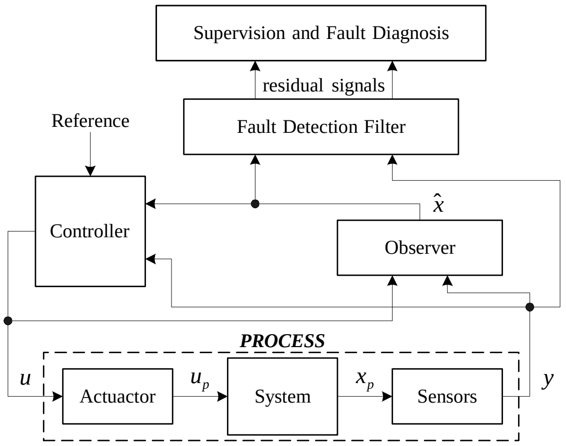

Fig. 1. Diagram of the fault tolerant control system considering fault diagnosis and supervision.

The model-based fault detection module utilizes the analytical redundancy, inherent in all dynamic relationships involving inputs and outputs of a system, in order to derive residuals corresponding to the expected faults. They could then be detected if residuals exceed a given threshold. To enable their isolation, a set of residuals are used, each one associated with a different kind of fault. Surveys can be found for instance in Frank and Ding (1997), Chen and Patton (1999) and Mangoubi and Edelmayer (2000).

Within a supervisory system residuals can be used to generate specific alarms and for monitoring the closed loop system's robustness as well. The diagram of a fault tolerant control system considering fault diagnosis and supervision is represented in Fig. 1. The overall control system provided by these methodologies will improve the plant efficiency and the closed loop performance as well as the robustness in presence of faults and disturbances. The proposed fault-tolerant control system was tested on a Distributed Solar Collector field (DSC).

2. EXTENDED MPC FORMULATION

Model-based predictive control is a discrete-time technique where an explicit dynamic model of the plant is used to predict the system's outputs over a finite prediction horizon *P* when control actions are manipulated throughout a finite control horizon *M*. At time step *k*, the optimiser computes on-line the optimal open-loop sequence of control actions such that the predicted outputs follow a pre-specified reference signal and taking into account possible hard and soft constraints. Only current control actions $u(k|k)$ are actually fed to the plant over the time interval $[k,k+1)$. Next, at time step $k+1$, the prediction and control horizons are shifted ahead by one step and a new optimisation problem is solved using the most recent measurements, and the control action fed to the plant in the previous time interval, $u(k|k)$.

Let the linearised discrete-time dynamics of a general non-linear system be described in the state-space form as follows:

$$\begin{aligned} x(k+1) &= \Phi x(k) + \Gamma u(k) + \eta \\ y(k) &= \Xi x(k) \end{aligned} \tag{1}$$

where $\Phi \in \Re^{n\times n}$, $\Gamma \in \Re^{n\times m}$ and $\Xi \in \Re^{p\times n}$ are, respectively, the state, input and output matrices; $x \in \Re^n$ is the state vector, $u \in \Re^m$ is the control vector and $y \in \Re^p$ the output vector; $\eta \in \Re^n$ is a constant vector related to the first term of the Taylor expansion, which is zero at any equilibrium point.

Considering a 2-norm for the cost functional and linear constraints on the inputs and outputs of the system and, additionally, bounds on the rate of change of control actions, the open-loop optimisation problem can be stated in the following way:

$$\begin{aligned} \min_u J = \min_u \Bigg\{ & \sum_{i=1}^{P} \left\| y(k+i\,|\,k) - r(k+i) \right\|_{Q_i}^2 + \\ & + \sum_{i=0}^{P-1} \left\| u(k+i\,|\,k) \right\|_{R_i}^2 + \sum_{i=0}^{M-1} \left\| \Delta u(k+i\,|\,k) \right\|_{S_i}^2 \Bigg\} \end{aligned} \tag{2}$$

subject to system dynamics (1) and to the following inequalities:

$$\begin{aligned} & y_{\min} \le y(k+i|k) \le y_{\max}, \quad i = 1,\ldots,P, \quad k \ge 0 \\ & u_{\min} \le u(k+i|k) \le u_{\max}, \quad i = 0,\ldots,P-1, \quad k \ge 0 \\ & \left| \Delta u(k+i|k) \right| \le \Delta u_{\max}, \quad i = 0,\ldots,M-1, \quad k \ge 0 \\ & \left| \Delta u(k+i|k) \right| = 0, \quad i = M,\ldots,P-1, \quad k \ge 0 \end{aligned} \tag{3}$$

with $Q_i \in \Re^{p\times p}$, $R_i \in \Re^{m\times m}$, $S_i \in \Re^{m\times m}$, $\Delta u \in \Re^m$ is the control increment vector and $r \in \Re^p$ is the reference signal.

Given the convexity of the optimisation problem any particular solution is a global optimum and thus the open-loop optimal control problem can be restated as a quadratic programming problem (4) and (5):

$$\textit{minimise} \qquad J(\Delta\tilde{u}) = h^T \Delta\tilde{u} + \frac{1}{2}\Delta\tilde{u}^T H \Delta\tilde{u} \tag{4}$$

$$\textit{Subject to} \qquad A^T \Delta\tilde{u} \le b \tag{5}$$

where $A \in \Re^{mM\times(4mM+2pP)}$, $b \in \Re^{(4mM+2pP)}$ and $\Delta\tilde{u} \in \Re^{mM}$ is the extended control increment vector over the control horizon.

In order to prevent from the effect of modelling errors, which accounts for static offsets, an offset compensator is incorporated into the control loop as depicted schematically in Fig. 2.

The filter works somehow as an integrator where the control error is previously weighted according to (6).

$$\alpha(k) = \frac{\kappa}{1 + \left[y(k) - r(k)\right]^2} \tag{6}$$

where $\kappa \in \mathbb{R}^+$.

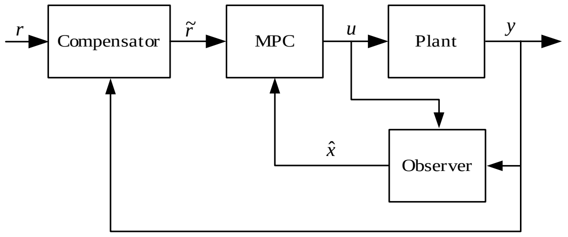

Fig. 2. Extended MPC Structure.

Next, this summation is added up to the true reference signal before being supplied to the MPC structure. Since the weighting factor α tends to zero beyond a narrow range from the set point the manipulation of the reference signal provided to the optimizer only takes place in the vicinity of the set point. This helps to prevent undesirable windup effects.

3. THE FAULT DIAGNOSIS MODULE

In model-based control techniques of non-linear systems by using local linear models it required a previous model linearization around operating points. The deviations between the linear model and the real plant will be assumed as uncertainties in the observer based detection module. For fault diagnosis purposes, the system's model also incorporates the actuator and sensor faults, which are described as additive signals.

The implementation of a *fault diagnosis system* will allow to detect, isolate and identify faults and to increase the robustness of the control system by collecting and analysing information on the system status using residual signals and other information sources. In order to enhance the prediction and decision making policies, neural networks and fuzzy logic techniques (see e.g. Zhang, *et al.* (2002)) may be combined with other techniques such as robust observers, parity space methods and hypothesis-testing methodologies.

4. DSC NEURAL MODELLING

The distributed solar collector field (DSC) is part of the Plataforma Solar de Almería (PSA), Fig. 3. It is a center for testing thermal solar energy applications, located on the desert of Tabernas, in the south of Spain.

The DSC field consists of 480 parabolic trough collectors arranged in 20 rows aligned on a West-East axis and forming 10 independent loops. Every solar collector has a linear parabolic-shaped reflector that focuses the sun's beam radiation on a linear absorber tube located at the focus of the parabola. Each of the loops is 172 *m* long, with an active section of 142 *m*, while the reflective area of the mirrors is around 264.4 m^2.

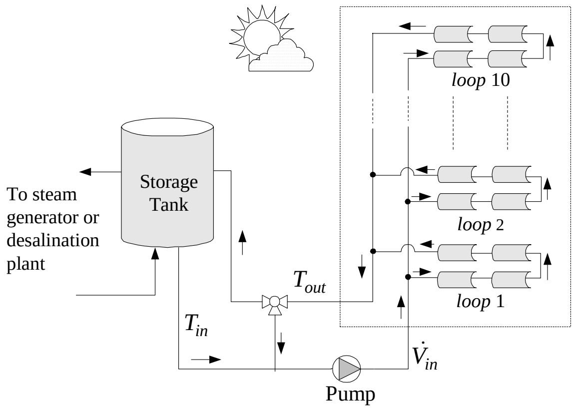

Fig. 3. Distributed solar collector field schematics.

The thermal oil is heated as it circulates through the absorber tube before entering the top of the storage tank. The colder inlet oil is extracted from the bottom of the tank. The thermal energy stored in the tank can be subsequently used to produce electrical energy in a conventional steam turbine/generator or in the solar desalination plant.

The plant modelling is carried out by means of a non-linear state space neural network being its general structure depicted in Fig. 4. This neural network structure can be described in the state space form by the following equations, assuming σ as a hyperbolic tangent function:

$$\begin{aligned} x(k+1) &= W_D \tanh\left(W_E x(k)\right) + W_A x(k) + W_B u(k) \\ x(0) &= x_0 \\ y(k) &= W_C x(k) \end{aligned} \tag{7}$$

where $x(k) \in \Re^{Nn}$ is the network internal hyperstate, $y(k) \in \Re^{No}$ is the network output, $u(k) \in \Re^{Ni}$ is the external input; Ni, Nn and No are, respectively, the number of neurons in the input layer, hidden layer and output layer.

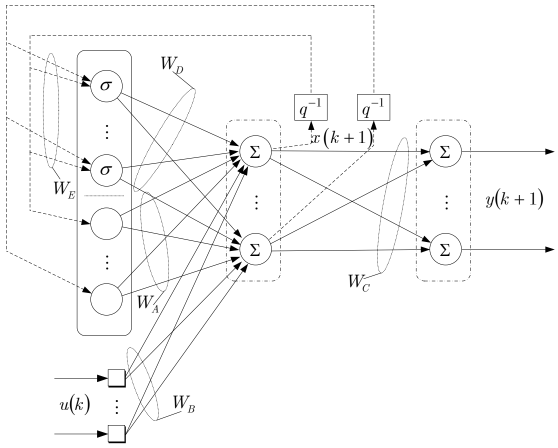

Fig. 4. Non-linear state-space neural network block diagram.

The synaptic weights between neurons, W_A, W_B, W_C, W_D and W_E, are real-valued matrices with appropriate dimensions. The predictor stability is assured for $\|W_A\|_2 + \max|e_{ij}|\|W_D\|_2 < 1$, where e_{ij} denotes the entries of matrix W_E, Gil, *et al*. (2004).

In the case of the DSC modelling, the input and the output layers both incorporate one neuron corresponding to the same number of inputs and outputs of the plant. The dimension of the state-space model was chosen as 2 according to a trade-off between the generalisation performance and the training error.

For the neural network training the present work follows a dual Kalman filter (DUKF) approach based on the unscented transformation (Julier, *et al.*, 2000). In the DUKF approach both states and weights are computed simultaneously in two stages: *i*) in the time update one step-ahead predictions are first computed, while *ii*) in the measurement update a correction is provided to these estimates on the basis of current noisy measurement. The dual Kalman filter equations are given by:

Weights estimation

Time update:

$$
\begin{aligned}
\Omega(k \mid k-1) &= \Omega(k-1 \mid k-1) \\
\mathrm{P}_{ww}(k \mid k-1) &= \mu^{-1}\mathrm{P}_{ww}(k-1 \mid k-1) \\
\mathcal{Z}^{w}(k \mid k-1) &= h\left(\hat{x}(k-1 \mid k-1), \Omega(k \mid k-1), k\right) \\
\hat{z}_w(k \mid k-1) &= \sum_{i=0}^{2Nw} \Gamma_i^w \mathcal{Z}_i^w (k \mid k-1)
\end{aligned}
\tag{8}
$$

Measurement update:

$$
P_{\nu\nu}^{w}(k \mid k-1) = \sum_{i=0}^{2Nw}\left\{\Gamma_i^w\left[\mathcal{Z}_i^w(k \mid k-1) - \hat{z}_w(k \mid k-1)\right]\left[\mathcal{Z}_i^w(k \mid k-1) - \hat{z}_w(k \mid k-1)\right]^T\right\} + R \tag{9}
$$

$$
\begin{aligned}
P_{wz_w}(k \mid k-1) &= \sum_{i=0}^{2Nw}\left\{\Gamma_i^w\left[\Omega_i(k \mid k-1) - \hat{w}(k \mid k-1)\right]\left[\mathcal{Z}_i^w(k \mid k-1) - \hat{z}(k \mid k-1)\right]^T\right\} \\
\mathcal{K}^w(k) &= \mathrm{P}_{wz_w}(k \mid k-1)\left(P_{\nu\nu}^w(k \mid k-1)\right)^{-1} \\
\hat{w}(k \mid k) &= \hat{w}(k \mid k-1) + \mathcal{K}^w(k)\left[z(k) - \hat{z}(k \mid k-1)\right] \\
\mathrm{P}_{ww}(k \mid k) &= \mathrm{P}_{ww}(k \mid k-1) - \mathcal{K}^w(k)\mathrm{P}_{\nu\nu}^w(k \mid k-1)\mathcal{K}^w(k)^T
\end{aligned}
$$

States estimation

Time update:

$$
\begin{aligned}
\mathcal{X}(k \mid k-1) &= f\left(\mathcal{X}(k-1 \mid k-1), u(k-1 \mid k-1), w(k-1 \mid k-1), k\right) \\
\hat{x}(k \mid k-1) &= \sum_{i=0}^{2Nn}\Gamma_i^x \mathcal{X}_i(k \mid k-1) \\
\mathrm{P}_{xx}(k \mid k-1) &= \sum_{i=0}^{2Nn}\Gamma_i^x\left[\mathcal{X}_i(k \mid k-1) - \hat{x}(k \mid k-1)\right] \\
\mathcal{Z}^x(k \mid k-1) &= h\left(\mathcal{X}(k \mid k-1), w(k-1 \mid k-1), k\right) \\
\hat{z}_x(k \mid k-1) &= \sum_{i=0}^{2Nn}\Gamma_i^x \mathcal{Z}_i^x(k \mid k-1)
\end{aligned}
\tag{10}
$$

Measurement update:

$$
\begin{aligned}
P_{\nu\nu}^x(k \mid k-1) &= \sum_{i=0}^{2Nn}\left\{\Gamma_i^x\left[\mathcal{Z}_i^x(k \mid k-1) - \hat{z}_x(k \mid k-1)\right]\left[\mathcal{Z}_i^x(k \mid k-1) - \hat{z}_x(k \mid k-1)\right]^T\right\} + R \\
P_{xz_x}(k \mid k-1) &= \sum_{i=0}^{2Nn}\left\{\Gamma_i^x\left[\mathcal{X}(k \mid k-1) - \hat{x}(k \mid k-1)\right]\left[\mathcal{Z}_i^x(k \mid k-1) - \hat{z}_x(k \mid k-1)\right]^T\right\} \\
\mathcal{K}^x(k) &= \mathrm{P}_{xz_x}(k \mid k-1)\left(P_{\nu\nu}^x(k \mid k-1)\right)^{-1} \\
\hat{x}(k \mid k) &= \hat{x}(k \mid k-1) + \mathcal{K}^x(k)\left[z(k) - \hat{z}(k \mid k-1)\right] \\
\mathrm{P}_{xx}(k \mid k) &= \mathrm{P}_{xx}(k \mid k-1) - \mathcal{K}^x(k)\mathrm{P}_{\nu\nu}^x(k \mid k-1)\mathcal{K}^x(k)^T
\end{aligned}
\tag{11}
$$

where μ denotes the forgetting factor, Ω the sigma points matrix of *w*, Γ the corresponding weight vector, $\mathcal{K}$ the Kalman gain and $\mathcal{X}$ the sigma points matrix of *x*.

5. RESULTS

The main control prerequisite in a DSC field is to maintain the outlet oil temperature at a prescribed value by suitably manipulating the oil flow rate through the receivers.

For this purpose, the proposed adaptive constrained non-linear MPC scheme with steady state offset compensation was tested on the Plataforma Solar de Almería DSC field. In all tests the sampling time was set to 15 seconds and the prediction horizon and the control horizon were chosen as $P = 10$ and $M = 1$ time steps.

In order to assess the robustness and fault tolerance properties of the proposed control scheme, some tests were carried out by injecting several specific faults and disturbances on sensors, actuator and on the system's parameters.

5.1 Adaptive NMPC

In this test an adaptive neural model-based predictive control without steady offset compensation was used for controlling the DSC field (Fig. 5).

The main goal with this experiment was to gather information upon the performance of the control system without any offset compensation and to get a reliable term of comparison for assessing the performance of the steady-state offset compensation approach. The initial covariance matrices involved in the weights adaptation computations were chosen as $P_{xx}(0)$=1 and $P_{ww}(0)$=$diag(5\times10^{-3})$ and the forgetting factor μ was set equal to 0.9986. In figure 5 it is shown the outlet oil temperature (T_{out}), set point (T_{ref}), oil flow rate through each DSC loop (Q_{in}), the inlet oil temperature (T_{in}) and the solar radiation (*Irr*).

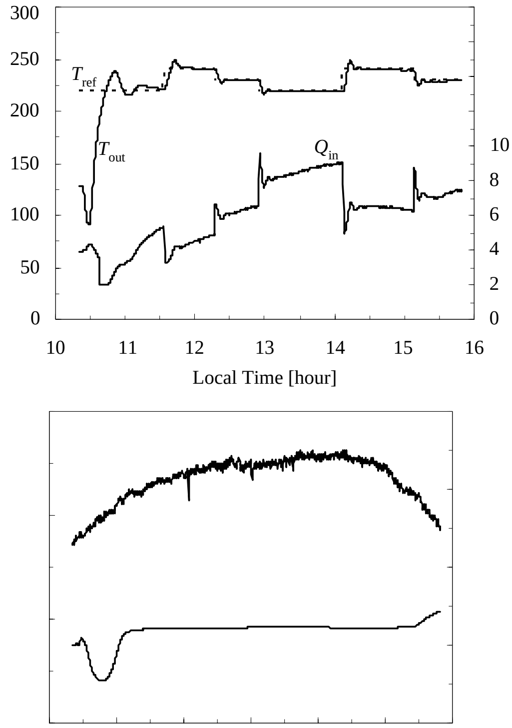

Fig. 5. ACUREX field test on the 17th July, 2002: Set point, outlet oil temperature and oil flow rate, solar radiation and inlet oil temperature.

As can be observed from the above plots, the adaptive MPC provides upon the whole a very acceptable response of the outlet oil temperature. Furthermore, as time goes on, as a result of increasing model accuracy the steady state errors become gradually lower. However, in view of the fact the adaptation mechanism is rather smooth when the solar radiation starts falling after noon the neural predictor becomes less accurate and so offset errors are once again observed. This new dynamics would be captured in case the test had not been stopped.

5.2 Adaptive NMPC plus Offset Compensation

This control test was carried out using an adaptive neural model-based predictive control incorporating a steady offset compensator (Fig. 6). The initial covariance matrices for the DUKF were chosen as $P_{xx}(0)$=1 and $P_{ww}(0)$=$diag(2\times10^{-3})$. Further, the forgetting factor was set equal to 0.9987 and $\kappa = 0.005$. Figure 6 shows the outlet oil temperature (T_{out}), set point (T_{ref}), oil flow rate through each DSC loop (Q_{in}), the inlet oil temperature (T_{in}) and the solar radiation (*Irr*). As can be observed from the above plots, this MPC scheme is able to drive the outlet oil temperature to the desired value even in the initial control stage where it is expected significant modelling errors. However, the price to pay is a more oscillating control system response.

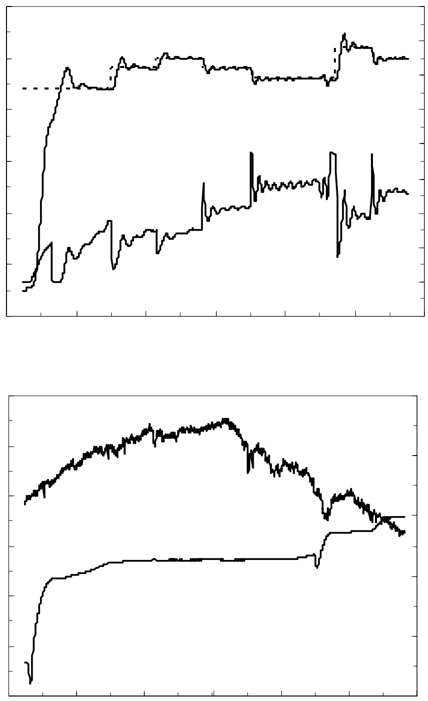

Fig. 6. ACUREX field test on the 23th July, 2002: Set point, outlet oil temperature and oil flow rate, solar radiation and inlet oil temperature.

5.3 Adaptive NMPC plus Offset Compensation in the Presence of Faults

This control test was carried out using an adaptive neural model-based predictive control incorporating a steady offset compensator, in the presence of some faults (Fig. 7). At 13:03 and at 13:07 the loops 6 and 4 were, respectively, disconnected, and at 13:53, these flow rates were re-established. From 14:36 to 15:03 a perturbation was introduced on the inlet temperature with maximum amplitude around 50ºC. At 15:10 an offset of +10ºC was added up to the outlet oil temperature for 16 minutes. At 15:37 an inlet oil temperature offset of +10ºC was injected for 9 minutes. Figure 7 shows the outlet oil temperature (T_{out}), set point (T_{ref}), oil flow rate through each DSC loop (Q_{in}), the inlet oil temperature (T_{in}) and the solar radiation (*Irr*).

As can be observed from these plots, the MPC scheme presents not only a quite good performance in driving the outlet oil temperature to the desired value but also a significant robustness considering the introduced faults. Actually, with this controller, the faults in system parameters (disconnection of loops) have almost no effects upon its behaviour. Regarding the perturbation on the inlet oil temperature it is noticed that it has a significant impact on the system's response. Nevertheless, the controller was effectively able to deal with this type of disturbances without a significantly deterioration of the overall performance.

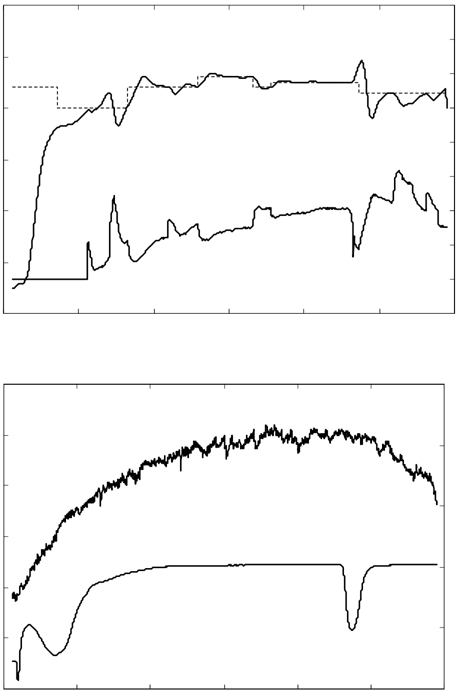

Fig. 7. ACUREX field test on the 31st July, 2002: Set point, outlet oil temperature and oil flow rate, solar radiation and inlet oil temperature.

For the two faults on the sensors, it must inferred that improvements should be considered by incorporating a fault diagnosis module and a supervisory system in order to detect, identify and accommodate these types of faults.

6. CONCLUSION

The paper reports the implementation of an adaptive constrained nonlinear model-based predictive control scheme with steady state offset compensation on a Distributed Solar Collector field at the Plataforma Solar de Almería. This approach was compared with an adaptive NMPC strategy without offset compensator so as to asses the overall control system robustness. Results show the feasibility of the proposed control scheme and its robustness to the tested faults.

ACKNOWLEDGEMENT

This work was partially supported by POSI– *Programa Operacional da Sociedade de Informação* of Portuguese Fundação para a Ciência e Tecnologia and by the European Union's FEDER and PRAXIS XXI ALCINE Projects. The experiments were carried under the support of the "Improving Human Potential" programme of EU-DGXII. The authors wish to express their gratitude to the PSA staff.

REFERENCES

Frank, P. M. and X. Ding (1997). Survey of robust residual generation and evaluation methods in observer-based fault detection systems. *Journal of Process Control*, **7(6)**, 403-424.

Chen, J. and R. J. Patton (1999). *Robust Model-Based Fault Diagnosis for Dynamic Systems*. Kluwer Academic Publishers.

Draeger, A., S. Engell and H. Ranke (1995). Model predictive control using neural networks. *IEEE Control Systems Magazine*, **15(5)**, 61-66.

Garcia, C., D. Prett and M. Morari (1989). Model predictive control: Theory and practice – a survey. *Automatica*, **25(3)**, 335-348.

Gil, P., J. Henriques, A. Dourado and H. Duarte-Ramos (2000). Constrained Neural Model Predictive Control with Guaranteed Free Offset. *Proc. 2000 IEEE Int. Conf. on IEECON*, 1991-1996.

Gil, P., J. Henriques, P. Carvalho, H. Duarte-Ramos and A. Dourado (2002). Adaptive Neural Model-Based Predictive Control of a Solar Power Plant. *IEEE International Joint Conference on Neural Networks*.

Gil, P., J. Henriques, A. Dourado and H. Duarte-Ramos (2004). Stability Analysis for a Class of Affine State-Space Neural Networks. *Proc. IEEE MED'2004*.

Hornik, K., M. Stinchcombe and H. White (1989). Multilayer Feedforward Networks are Universal Approximators. *Neural Networks*, **2**, 359-366.

Ichtev, A., J. Hellendoorn, R. Babuska and R. Mollov (2002). Fault-Tolerant Model-Based Predictive Control Using Multiple Takagi-Sugeno Fuzzy Models.. *Proceedings of FUZZ-IEEE'02, the 2002 IEEE International Conference on Fuzzy Systems*, **1**, 346–351.

Julier, S., J. Uhlmann and F. Durrant-Whyte (2000). A New Method for the Nonlinear Transformation of Means and Covariances in Filters and Estimators. *IEEE Trans. Aut. Control*, **45**, 477-482.

Mangoubi, R. S. and A. M. Edelmayer (2000). Model Based Fault Detection: The Optimal Past, the Robust Present and a Few Thoughts on the Future. *Proceedings of the IFAC Symposium SAFEPROCESS'2000*, 64-75.

Rivals, I. and L. Personnaz (1996). Black-box modelling with state-space networks. *Neural Adaptive Control Technology*, (R. Zbikowski and J. Hunt eds., World Scientific), 237-264.

Yamada, T. and T. Yabuta (1993). Dynamic System Identification Using Neural Networks. *IEEE Trans. On Systems, Man and Cybernetics*, **23(1)**, 204-211.

Zhang, X., M. Polycarpou, and T. Parisini (2002). A Robust Detection and Isolation Scheme for Abrupt and Incipient Faults in Nonlinear Systems. *IEEE Transactions on Automatic Control*, **47(4)**, 576-593.